Journal of Catalysis **184,** 514–525 (1999)
Article ID jcat.1999.2457, available online at http://www.idealibrary.com on IDEAL®

Characterization of Bimetallic PtSn Catalysts Supported on Purified and H_2O_2-Functionalized Carbons Used for Hydrogenation Reactions

S. R. de Miguel,* M. C. Román-Martínez,† E. L. Jablonski,* J. L. G. Fierro,‡ D. Cazorla-Amorós,† and O. A. Scelza*

*Instituto de Investigaciones en Catálisis y Petroquímica (INCAPE), Facultad de Ingeniería Química—Universidad Nacional del Litoral, CONICET, Santiago del Estero 2654, (3000) Santa Fe, Argentina; †Departamento de Química Inorgánica, Facultad de Ciencias, Universidad de Alicante, Apart. 99-E, Alicante, Spain; and ‡Instituto de Catálisis y Petroleoquímica, Campus Universidad Autónoma, Cantoblanco, 28049 Madrid, Spain
E-mail: oascelza@fiqus.unl.edu.ar, mcroman@ua.es

Received November 23, 1998; revised February 6, 1999; accepted February 6, 1999

The state of the metallic phase of PtSn/C catalysts prepared by coimpregnation and successive impregnation on purified and H_2O_2-functionalized carbons as supports was studied by TPD, TPR, H_2 chemisorption, XPS, and test reactions. Furthermore, the characteristics of the metallic structures were related with the catalytic behaviors in the selective hydrogenation reaction of carvone in liquid phase. In PtSn/C samples, most of the Sn would be in intimate contact with Pt, and the surface of the reduced bimetallic catalysts would be composed of metallic platinum, Sn(II), and/or Sn(IV) species, and small amounts of zerovalent tin, probably forming alloys with Pt^0. The high selectivity of these bimetallic PtSn/C catalysts for the production of unsaturated alcohols in the reaction of carvone hydrogenation would be due to the action not only of the promoter (Sn) but also of the support (carbon).

Key Words: **PtSn/C catalysts; selective hydrogenation of carvone; characterization of catalysts.**

INTRODUCTION

The effect of tin addition to Pt was extensively studied during the last years in catalysts for different processes such as naphtha reforming and dehydrogenation of heavy and light paraffins, and more recently for hydrogenation reactions in liquid phase. These PtSn bimetallic catalysts, mainly supported on alumina and silica, show a good performance both in selectivity and stability in these reactions. There is much of information about the correlation between the surface characteristics and the catalytic properties of this bimetallic system supported on different metallic oxides (1–10). The metallic structures of these bimetallic catalysts, prepared by different methods, were characterized by means of different techniques like TPR, diffuse reflectance, FT-IR, X-ray diffraction, XPS, EXAFS, Mössbauer, and electron microdiffraction. In general, the use of inert supports such as SiO_2 leads to catalysts with a weak metal–support interaction (6, 9), in this way favoring the formation of PtSn alloy phases. On the contrary, the use of supports which strongly interact with the metals leads to catalysts with a lower presence of intermetallic alloys (3, 4). In this last case, besides the electronic interaction, other phenomena like geometric or dilution effects and surface Sn-enrichment would be present (4).

On the other hand, the bimetallic PtSn system supported on activated carbon has been studied by few authors (11–13). In this sense, Coloma *et al.* (11, 12) found, by using gas chemisorption, XPS, and crotonaldehyde hydrogenation reaction, the presence of both metallic and oxidized tin species in the reduced catalysts, and postulated that the selectivity to the hydrogenation of the carbonyl group seems to be related to the relative amount of oxidized surface tin species. Furthermore, Pinxt *et al.* (13) found by EXAFS that the reductive treatment with hydrogen at high temperatures (300°C) reduced all platinum and a fraction of tin. According to these EXAFS results (13), platinum showed Pt–Pt, Pt–C, and Pt–Sn coordination, and tin displayed Sn–Pt and Sn–O coordination, thus indicating the tin interaction both with platinum and, via oxygen, with the graphite support.

In this paper, a complete characterization of dried and reduced monometallic Pt/C and Sn/C and bimetallic PtSn/C catalysts is carried out in order to study the state of the metallic phase. Bimetallic catalysts were prepared by two different impregnation procedures and using two carbon supports with different surface chemistry. The characterization techniques used for this study were TPR, TPD, XPS, H_2-chemisorption measurements, and two test reactions of the metallic phase (cyclohexane dehydrogenation and cyclopentane hydrogenolysis). Finally, a relationship between the states of the metallic phase of Pt/C and PtSn/C catalysts and their catalytic behavior in the carvone hydrogenation in liquid phase, mainly in the selective activation of the carbonyl group, is introduced in this paper.

0021-9517/99 $30.00

EXPERIMENTAL

A commercially derived pit of peach carbon (GA-160 from Carbonac) was used as a support. This carbon was crushed and sieved to a final particle size between 100 and 140 mesh. Since the impurities content of this carbon was 2.9 wt% (K, 1.23; Ca, 0.41; Na, 0.46; Mg, 0.07; Si, 0.12; P, 0.09; Fe, 0.09; Cl, 0.44; S, 0.03 wt%), this material was purified by successive treatments with aqueous solutions (10 wt%) of HCl, HNO_3, and HF at room temperature during 48 h. After HCl and HNO_3 treatments, the carbon was repeatedly washed with deionized water up to a final pH 4, and after the HF treatment, it was washed with deionized water up to a final pH 7. Finally, it was dried at 120°C during 24 h. The acid-treated carbon was submitted to a thermal treatment with 5 ml of H_2 min^{-1} g^{-1} at 850°C during 8 h. After the acid and thermal treatments, the inorganic impurities decreased up to 0.16 wt% (K, 0.03; Ca, 0.06; Na, 0.008; Mg, 0.009; Si, 0.009; P, 0.009; Fe, 0.03; Cl, 0.005 wt%; S, undetectable). The analysis of the impurities of the starting and the acid treated carbon was carried out by EDX on the ashes, which were obtained by total burn-off of carbons with air at 500°C in an electric furnace. The purified carbon was labeled as "C." A fraction of this carbon was subsequently submitted to functionalization treatments with H_2O_2 aqueous solution (20 v/v %) at room temperature during 48 h. The H_2O_2-functionalized carbon, named as CP-HP, was dried at 120°C during 24 h.

Precursors of bimetallic PtSn/carbon catalysts were prepared by two different impregnation sequences: (a) coimpregnation (C) of carbon with an aqueous solution of H_2PtCl_6, $SnCl_2$, and HCl (0.4 M), and (b) two-step or successive impregnation (SI) of the carbon, first with a solution containing $SnCl_2$ and HCl (0.4 M) followed by a drying step at 120°C, and second with an aqueous solution of H_2PtCl_6. Precursors of monometallic Pt/carbon and Sn/carbon were also prepared. In all cases, the ratio between the volume of impregnating solution and the carbon weight was 30 ml g^{-1} and the impregnation procedure was as follows. The supports were maintained in contact with the impregnating solution under stirring at 25°C during 5 h. The solid was then separated by filtration and dried at 120°C during 24 h. The platinum and tin loadings in the different catalysts are collected in Table 1.

The characterization of the porous structure of carbons was carried out by physical adsorption of N_2 at −196°C by using a Micromeritics ASAP 2000 apparatus.

Temperature-programmed experiments (TPD and TPR) were carried out in an apparatus consisting, basically, of a differential flow reactor coupled to a mass spectrometer. In both cases, approximately 200 mg of sample was heated in an electric furnace at a heating rate of 50°C min^{-1} from room temperature up to 950°C. During the TPD experiments, He was passed through the reactor with a flow rate equal to 60 ml min^{-1}. For TPR experiments, a mixture of 5% H_2 in He with a flow rate of 60 ml min^{-1} was used. The gas analysis was carried out by mass spectrometry.

TABLE 1

Pt and Sn Loadings and Pt/Sn Molar Ratios of the Different Catalysts

Catalyst	wt% Pt	wt% Sn	Pt/Sn molar ratio
Pt/C	0.85		
Pt/C-HP	0.84		
Sn/C		0.43	
Sn/C-HP		0.45	
PtSn/C (C)	0.78	0.36	1.32
PtSn/C (SI)	0.86	0.42	1.25
PtSn/C-HP (C)	0.81	0.38	1.30
Pt/C-HP (SI)	0.89	0.39	1.38

X-ray photoelectron spectra (XPS) were obtained by using a Fisons ESCALAB MkII 200R electron spectrometer fitted with a Mg$K\alpha$ (1253.6 eV) source operated at 12 kV and 10 mA and equipped with a hemispherical electron analyzer. XPS measurements were carried out both on dried samples and on samples previously treated "*in situ*" with H_2 at 350°C. The ion pumper analysis chamber was maintained below 10^{-9} Torr during the data acquisition. The Sn/Pt surface ratios were calculated from the peak areas normalized by published atomic sensitivity factors (14). Peak areas were estimated by calculating the integral of each peak after subtraction of the S-shaped background and fitting the experimental peak by a combination of Lorentzian/Gaussian (L/G) curves of variable proportion. This L/G proportion was fixed to zero for the Pt 4*f* core levels of H_2-reduced samples. Binding energies (eV) of core levels were referenced to the BE of C 1*s* peak at 284.9 eV.

The H_2 chemisorption measurements were carried out at 25°C in a volumetric equipment. The catalyst was reduced with H_2 at 350°C during 4 h, and then it was outgassed under high vacuum (10^{-4} Torr) at 350°C for 1 h. When the sample was cooled down to room temperature, the chemisorption test began.

The catalytic activity for cyclohexane (CH) dehydrogenation was determined at 300°C and at atmospheric pressure in a differential flow reactor by using a H_2/CH molar ratio of 29 and a CH molar flow of 0.056 mol h^{-1}. The activation energy of this reaction was obtained by measuring the catalytic activity at 270, 285, and 300°C. The conditions for the cyclopentane (CP) hydrogenolysis were $T = 400$°C, H_2/CP molar ratio = 25, and CP molar flow = 0.064 mol h^{-1}. The sample weight used in these experiments was the appropriate to obtain a CH or CP conversion lower than 7%. The reaction products were only benzene and *n*-pentane for the first and second reactions, respectively. The products of both reactions were analyzed by using a gas chromatographic system.

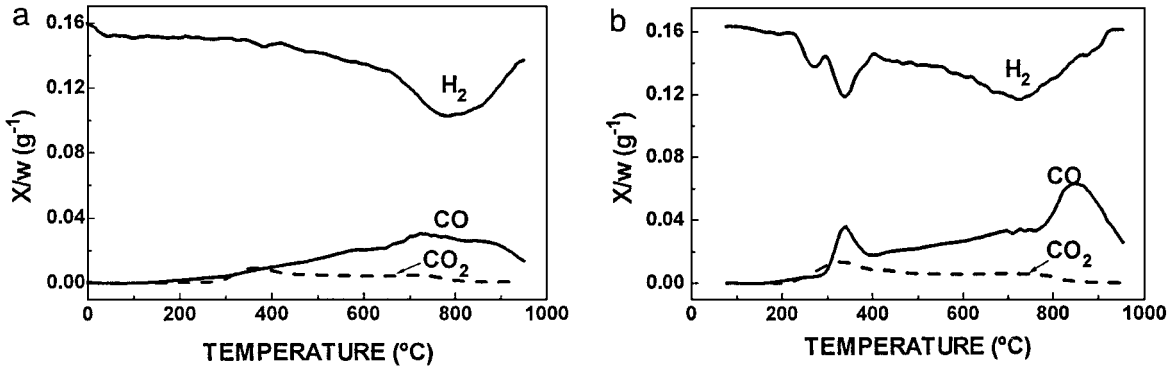

FIG. 1. (a) TPR profiles of C-HP sample. (b) TPR profiles of Pt/C-HP catalyst.

The carvone hydrogenation reaction was carried out at 40°C and atmospheric pressure in a discontinuous volumetric reaction equipment, by using toluene as a solvent and a stirring rate of 360 rpm. In each experiment, 0.09 g of carvone dissolved in 30 cm^3 of toluene was hydrogenated by using 0.40 g of catalyst. Before the reaction, catalysts were reduced "*in situ*" with H_2 at 350°C during 3 h, and then they were cooled down to the reaction temperature. H_2 was then introduced into the reactor. After a stabilization period, carvone solution (in toluene), prepared without contact with air, was injected to the reactor, thus beginning the reaction. The reaction conditions were selected to avoid diffusion limitations. Reaction products were intermittently withdrawn from the reactor and analyzed in a GC chromatographic system with a capillary column (Supelcowax 10 M).

RESULTS AND DISCUSSION

Textural and TPD Results of Carbons

Data of textural properties and surface chemistry of supports, determined by N_2 adsorption and TPD experiments, respectively, are shown in Table 2. As can be observed, the functionalization treatment of carbons with hydrogen peroxide produces a slight increase in the amount of groups desorbing CO_2 and an important increase in the concentration of groups desorbing CO, compared with the purified carbon (C). On the other hand, there is practically no influence of the H_2O_2 functionalization treatment on the physical properties of the carbons.

TABLE 2

Textural Characteristics and Amounts of Desorbed CO_2 and CO During TPD Experiments on the Supports

Support	S_{BET} ($m^2\ g^{-1}$)	$V_{micropores}$ ($cm^3\ g^{-1}$)	Desorbed CO_2 (μmol/g)	Desorbed CO (μmol/g)
C	976	0.33	91	259
C-HP	890	0.29	133	663

TPR and TPD

Figures 1a and 1b show TPR profiles of the carbon functionalized with H_2O_2 (C-HP) and of the catalyst precursor Pt/C-HP after impregnation and drying steps, respectively. The TPR profile of the support (Fig. 1a) shows only one H_2 consumption zone at high temperature, between 500 and 900°C, while three H_2 consumption zones can be clearly observed for the Pt catalyst (Fig. 1b). The H_2 consumption zone at high temperatures ($T > 500$°C) appears both for the catalyst and the carbon (Figs. 1a and 1b), and it has been attributed to the interaction of H_2 with reactive surface sites created by decomposition of functional groups (mainly those that evolve CO) (15, 16). The first H_2 consumption peak (with a maximum at 265–270°C) observed in the TPR profile of the catalyst (Fig. 1b) would correspond to the reduction of the deposited metal complex, in agreement with previous works dealing with Pt catalysts supported on carbons with different surface oxidation degree (16). The second H_2 consumption peak (Fig. 1b) with a maximum at about 360°C is coincident with the maximum in the CO_2 desorption peak and a with a well-defined CO-desorption peak observed at 360°C in the same TPR experiments. It seems that hydrogen is consumed by the interaction with reactive surface sites created by CO_2 and CO evolutions at this relatively low temperature. It must be noted that the CO-desorption peak at low temperature was not found in TPR profiles of the corresponding support (Fig. 1a), but it was observed in TPD experiments carried out with dried Pt/C and Pt/C-HP samples (15). These observations suggest that this CO peak at low temperature should be related to the decomposition of surface groups formed during the impregnation step by a red-ox process between the metal precursor and the carbon surface for both Pt/C and Pt/C-HP samples (15). Evidence of the partial reduction of $PtCl_6^{2-}$ upon interaction with the carbon surface has already been found by different authors by using different techniques

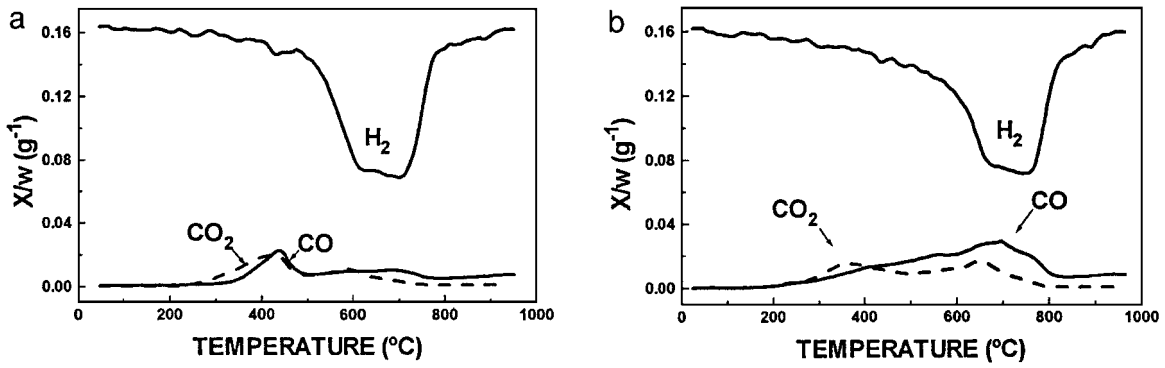

FIG. 2. (a) TPR profiles of Sn/C sample. (b) TPR profiles of Sn/C-HP sample.

(XPS, TPR, TPD, and EXAFS) (15–18). Moreover, it must be noted that the CO amount produced by the interaction of $PtCl_6^{2-}$ was found to increase for H_2O_2-functionalized carbons with respect to that of nonfunctionalized one (15).

Figures 2a and 2b show TPR profiles of Sn/C and Sn/C-HP precursors, respectively. Besides, the H_2 consumption and HCl desorption profiles corresponding to the TPR experiment of the bulk Sn precursor ($SnCl_2 \cdot 2H_2O$) are shown in Fig. 3. The reduction of bulk $SnCl_2$ happens in two steps, revealed by two hydrogen consumption peaks (at 650 and 800°C), which are accompanied by a HCl desorption zone. On the other hand, the H_2 consumption in both Sn/C precursors (Figs. 2a and 2b) shows one large peak between 500 and 850°C. It must be noted that a small and narrow HCl desorption peak was observed between 500 and 600°C, thus indicating the decomposition and probable reduction of the Sn-chlorinated precursor at these temperatures. The oxidation state of tin in the dried samples is yet unclear. In fact, the drying step after impregnation could modify the tin oxidation state. In this sense the literature reveals that Sn^{2+} can be oxidized to Sn^{4+} in samples supported on alumina (19). The hydrogen consumption found for both samples (Sn/C and Sn/C-HP) in TPR experiments corresponds to approximately 28 mol H_2/mol Sn. This amount is much higher than is necessary for the total reduction from Sn^{4+} (maximum oxidation state of Sn) to Sn^0 (2 mol H_2/mol Sn), and in consequence the remaining H_2 consumption would be due to an additional effect such as a large H_2 retention on the carbon surface.

The temperature at which the hydrogen consumption takes place in both Sn/C samples indicates that the presence of metallic tin could be an important factor for the H_2 retention on the carbon. However, results obtained from additional experiments lead to the hypothesis that the presence of surface oxidized groups can also play a very important role. In fact, a TPR experiment (Fig. 4) carried out on a Sn/C-HP sample after a He treatment at 900°C (conditions at which the oxidized groups are practically destroyed) shows a small amount of consumed H_2 at 550–600°C (about 3 mol H_2/mol Sn). This amount is close to the necessary for the total reduction of Sn to the metallic state. In these conditions, the H_2 retention by the support is very low, in spite of the presence of metallic Sn. These results would indicate that in the absence of oxidized surface groups, the H_2 retention strongly decreases. The participation of zerovalent metals in the H_2 retention has been reported in the

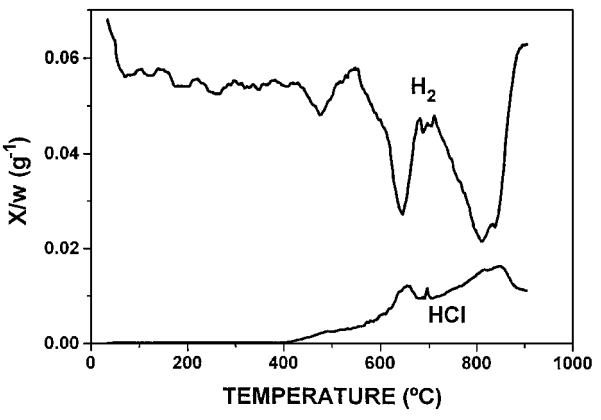

FIG. 3. TPR profiles of bulk $SnCl_2 \cdot 2H_2O$ compound.

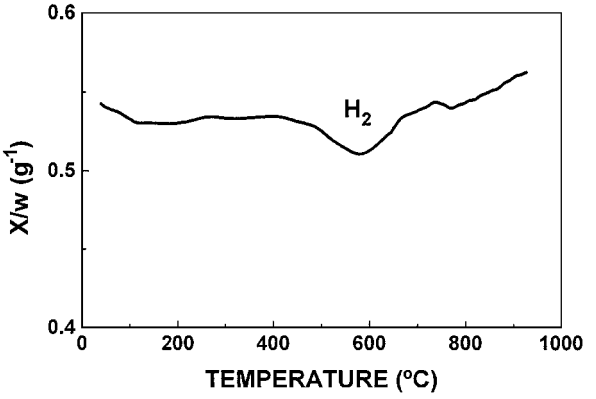

FIG. 4. TPR profile (H_2 consumption) of Sn/C-HP sample after a thermal treatment in a He stream at 900°C.

literature for Pt/C catalysts (5, 15). In this case, H_2 (previously dissociated on the metal) can interact with the carbon surface by combining with reactive sites developed by decomposition of functional groups. Thus, it can be concluded that the presence of both metallic tin and surface functional groups would determine the large retention of H_2 in the Sn/C and Sn/C-HP samples. Besides, the tin deposition on carbon also produces a modification of the distribution of functional groups within the structure of carbons as it can be seen through the comparison of CO and CO_2-desorption profiles (obtained in TPR experiments) of Sn/C samples (Figs. 2a and 2b) with those of the corresponding support (Fig. 1a) and of the Pt/C sample (Fig. 1b). Thus, the CO evolutions for Sn/C samples are shifted to lower temperatures compared with those of the corresponding supports and of the monometallic Pt catalysts. This fact could be explained considering that the presence of Sn in the proximity of oxygen functional groups favors their decomposition at lower temperatures.

Figures 5a–d show the TPR profiles of bimetallic PtSn/C (SI), PtSn/C (C), PtSn/C-HP (SI), and PtSn/C-HP (C), respectively. In the first place, it must be pointed out the important differences between the TPR profiles of these samples compared with those found for both monometallic catalysts (Figs. 5, 1b, and 2). Thus, a first well-defined hydrogen consumption zone is localized between 200 and 500°C for the four bimetallic catalysts, though in the case of PtSn/C-HP (C), this reduction zone appears divided in two peaks (Fig. 5d). There is also a broad H_2 consumption zone between 500 and 950°C. The consumed hydrogen amounts between 200 and 500°C are about 7 mol H_2/mol (Pt + Sn). A fraction of these H_2 amounts can be assigned to the co-reduction of platinum and tin, since the maximum H_2 amount necessary for the total reduction of both metals is 4 mol H_2/mol (Pt + Sn). Hence, the remaining consumed H_2 amount (3 mol H_2/mol (Pt + Sn)) could be retained on the carbon surface. In conclusion, it seems that tin is reduced at lower temperature due to the presence of platinum, and that an important H_2 retention on the carbon surface would take place. The consumed H_2 amount above 500°C in bimetallic catalysts is similar to those observed in the TPR experiments with carbons and Pt/C-HP sample (Figs. 1a, 1b, and 5), but much lower than the large H_2 consumption found for Sn/C and Sn/C-HP samples at high temperature (Fig. 2). These results indicate that practically no free Sn species are detected in bimetallic catalysts by TPR measurements.

It must be pointed out that the TPR profiles of the bimetallic samples (Fig. 5) also show CO-desorption peaks at low temperatures (250–400°C). As it was explained above, this CO peak also appears in the TPR of monometallic Pt catalysts (Fig. 1b), but it was not found in that of carbon (Fig. 1a). In consequence, it seems that during the impregnation step, Pt is partially reduced by contact with

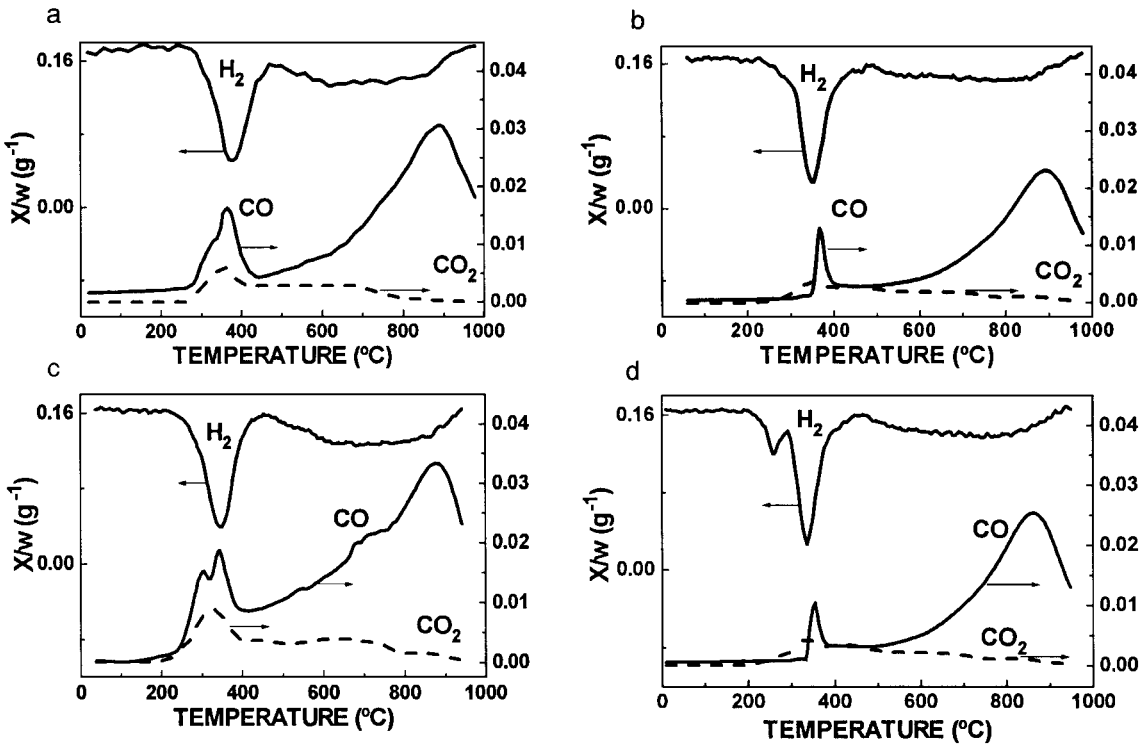

FIG. 5. TPR profiles of (a) PtSn/C (SI); (b) PtSn/C (C); (c) PtSn/C-HP (SI); and (d) PtSn/C-HP (C).

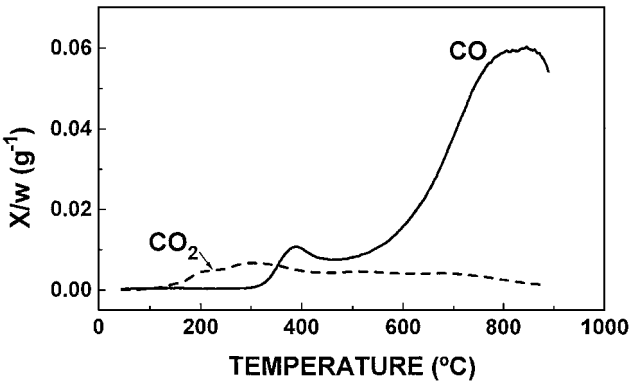

FIG. 6. TPD profiles of the PtSn/C-HP (SI) sample.

carbon (15), and this red-ox process originates some functional groups on the support surface. These groups would decompose at low temperature (during TPR), thus developing reactive sites for the hydrogen interaction. TPR results show that the presence of tin does not hinder this process, though there are some differences in the distribution of surface oxygen groups in the case of successively impregnated samples. This is revealed by the shape of the CO evolution at low temperature (Figs. 5a and 5c). More evidence about the development of new surface functional groups during the impregnation and drying steps (via red-ox processes) can be obtained by comparing the TPD profiles of the PtSn/C-HP (SI) sample (Fig. 6) with the TPR profiles of the same sample (Fig. 5c). In this sense, the first CO-desorption peak (between 200 and 400°C) in the TPR experiment is detected at lower temperatures than that observed in the TPD, moreover the intensity of the TPR peak is higher than that found in the desorption experiment. This fact reveals that hydrogen in the presence of Pt metallic particles enhances the decomposition of surface oxygen complexes by spillover of hydrogen from metal toward the carbon surface. This behavior was also reported by other authors (16, 20).

It must be noted that the formation of small amounts of methane was also observed during TPR experiments. The profiles of the methane evolution of mono and bimetallic catalysts supported on the H_2O_2-functionalized carbon have been compared in Fig. 7 with the one corresponding to the support. Methane is desorbed at high temperature (≥800°C) from C-HP and Sn/C-HP, and the evolved CH_4 amounts were 8 and 11 μmol/g, respectively. On the other hand, methane evolution from Pt/C-HP is much higher (41 μmol CH_4/g) and a maximum appears at 650°C. Finally, there are also important amounts of desorbed CH_4 (23 and 18 μmol CH_4/g for the (SI) and (C) catalysts, respectively) for bimetallic samples, but they are lower than that of Pt/C-HP and appear at slightly higher temperatures (700°C). These results clearly indicate the catalytic effect of Pt on the methane formation in Pt/C catalysts. When Sn is added to Pt/C, it modifies the metallic phase, noticeably reducing the catalytic activity for methane formation.

XPS

Table 3 shows the binding energies of the Pt $4f_{7/2}$ and Sn $3d_{5/2}$ levels for the four bimetallic PtSn catalysts, both after the drying step and after the reduction treatment at 350°C. Figures 8 and 9 display the Pt 4*f* and the Sn 3*d* signals for dried and reduced bimetallic catalysts, respectively. From the deconvolution of the Pt 4*f* XPS spectra of dried samples (Fig. 8), two peaks were obtained: one with a low binding energy at 72.0–72.1 eV, which can be assigned to metallic platinum, and a second one at 73.5–73.9 eV, which corresponds to a Pt(II) chlorinated species (Table 3). The appearance of Pt(II) and Pt(0) species in these dried PtSn/carbon samples could be due to a red-ox reaction during the impregnation step (as it has already deduced from

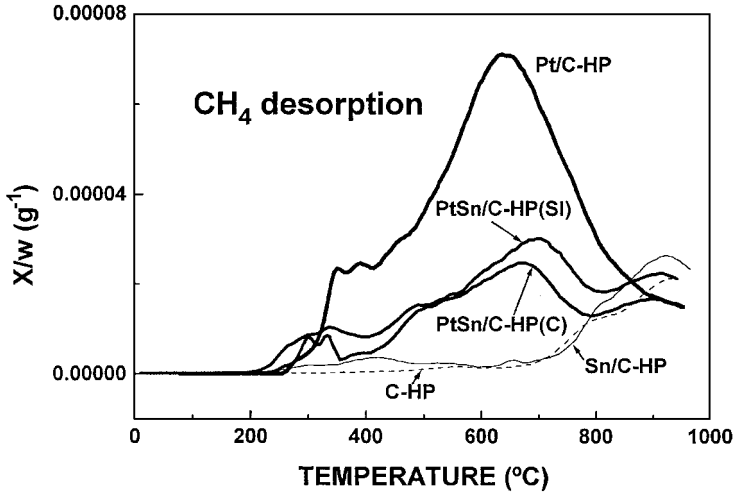

FIG. 7. Desorption profiles of methane during TPR experiments on different catalysts.

TABLE 3

Binding Energies (eV) and Sn/Pt Surface Atomic Ratios in the XPS Measurements on Dried and Reduced Catalysts

Catalyst	BE Pt $4f_{7/2}$ (eV)		BE Sn $3d_{5/2}$ (eV)		Sn_T/Pt_T atomic surface ratio
	After drying	After reduction	After drying	After reduction	
PtSn/C (C)	72.0 (54%)	71.8		486.4 (17%)	16.1
	73.7 (46%)		487.7	487.7 (83%)	
PtSn/C-HP (C)	72.1 (53%)	71.7		486.1 (13%)	23.3
	73.9 (47%)		487.8	487.7 (87%)	
PtSn/C (SI)	72.0 (62%)	71.8		486.3 (12%)	24.4
	73.9 (38%)		487.7	487.7 (88%)	
PtSn/C-HP (SI)	72.0 (57%)	71.9		486.5 (13%)	27
	73.5 (43%)		487.8	487.7 (87%)	

[a] Numbers in parentheses correspond to peak percentages.

TPR and TPD experiments, see above). On the contrary, XPS spectra of the four reduced PtSn bimetallic catalysts (Fig. 9) show a single peak around 71.8 eV, which indicates that Pt is completely reduced to zerovalent state after H_2 reduction at 350°C. Similar XPS results corresponding to Pt signals were found by Coloma *et al.* in a previous study (12). It can be noted in Fig. 9 (Pt 4*f* lines) that an additional peak close to 76 eV, assigned to Al 2*p* level of aluminium oxide impurities, was introduced in order to obtain good fittings. In no case this component arises from Pt because the Pt $4f_{5/2}$/Pt $4f_{7/2}$ intensity ratio rule must be maintained.

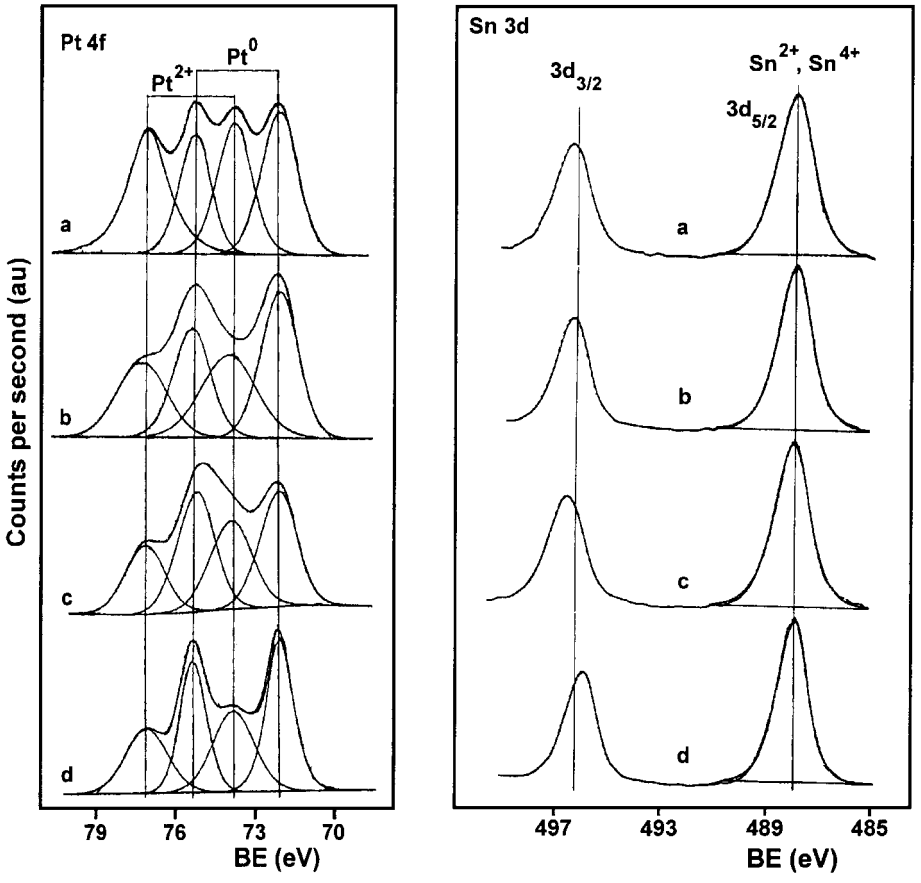

FIG. 8. XPS spectra corresponding to Pt 4*f* and Sn 3*d* signals on dried samples: (a) PtSn/C (C); (b) PtSn/C (SI); (c) PtSn/C-HP (C); (d) PtSn/C-HP (SI).

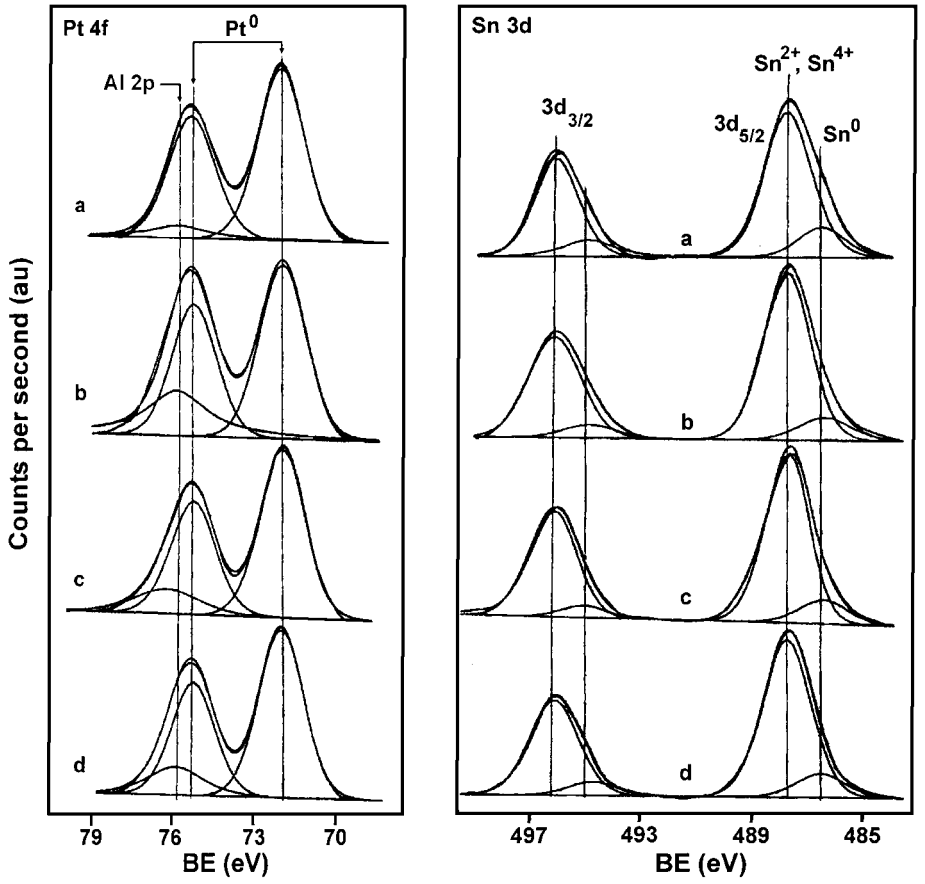

FIG. 9. XPS spectra corresponding to Pt 4*f* and Sn 3*d* signals on reduced samples: (a) PtSn/C (C); (b) PtSn/C (SI); (c) PtSn/C-HP (C); (d) PtSn/C-HP (SI).

The Sn 3*d* XPS spectra of the dried samples show a peak at 487.7–487.8 eV corresponding to Sn(II) and/or Sn(IV) species (Table 3). It must be noted that the distinction between Sn(II) and Sn(IV) species from XPS results is not possible since both species have a very small difference in the binding energy (21). From the deconvolution of the Sn 3*d* signals of reduced bimetallic samples (Fig. 9), two peaks were observed: the first one at 487.7–487.8 eV, corresponding to Sn(II) and/or Sn(IV) species, and the second one at 486.1–486.5 eV, characteristic of metallic tin. In all cases the percentages of zerovalent tin ranges between 12 and 17% of the total tin species (Table 3). In conclusion, we can say that the surface of the reduced bimetallic catalysts is composed of metallic platinum, Sn(II) and/or Sn(IV) species in high concentrations, and small amounts of zerovalent tin, which could be forming alloy phases with metallic Pt. Previous results of an on-line characterization by EXAFS of PtSn supported on graphite reduced with H_2 at 573 K showed both the tin bonding (via oxygen) to the support and the PtSn alloy formation (13).

Table 3 also shows the values of surface atomic ratios between the total Sn and the total platinum (Sn_T/Pt_T). These values range between 16 and 27 Sn atoms/Pt atom, thus indicating a very important Sn surface enrichment in these bimetallic catalysts supported on carbons. This Sn enrichment, but in a much lower extension (≈3 Sn surface atoms/Pt surface atom), was also observed in PtSn catalysts supported on Al_2O_3 (22).

H_2 Chemisorption

Table 4 shows the amounts of chemisorbed hydrogen (H/M, mmol H_2/g Pt) on the different mono and bimetallic catalysts. Results obtained with this technique show the following trend in the chemisorption capacity:

$$\text{Pt/C-HP} > \text{Pt/C} > \text{PtSn/C (SI)} > \text{PtSn/C-HP (SI)} > \text{PtSn/C (C)} \cong \text{PtSn/C-HP (C)}$$

According to these results, the tin addition to Pt decreases the chemisorption capacity, probably due both to an electronic effect between both metals (with possible alloy formation) and to geometric effects (dilution and Pt blocking by Sn). These effects appear to be more pronounced in co-impregnated catalysts. In this case, a reaction between

TABLE 4

H_2-Chemisorption Values (H/M) and Initial Reaction Rates (r_0) of Cyclohexane (CH) Dehydrogenation and Cyclopentane (CP) Hydrogenolyis

Catalyst	H/M (mmol H_2/g Pt)	r_0 (mol h^{-1} g Pt^{-1})		$E_{A,CH}$ (kcal/mol)[a]
		CH	CP	
Pt/C	1.01	32.0	1.7	19.6
Pt/C-HP	1.15	86.2	1.97	21.6
PtSn/C (C)	0.57	2.2	0	29.4
PtSn/C-HP (C)	0.57	9.9	0	30.1
PtSn/C (SI)	0.75	3.0	0	28.8
PtSn/C-HP (SI)	0.68	7.7	0	26.1

[a] $E_{A,CH}$ is the activation energy of cyclohexane dehydrogenation.

both metallic precursors in the impregnating solution would lead to a high concentration of a PtSn complex, $(PtCl_2(SnCl_3)_2)^{2-}$, where Pt and Sn are in intimate contact. This complex was isolated from the impregnating solution according to the technique described by Antonov *et al.* (23) and it was identified by using diffuse reflectance spectroscopy (DRS). The Pt–Sn complex can be considered as the precursor of Pt–Sn alloys during the subsequent thermal treatments. A similar behaviour was previously observed in $PtSn/Al_2O_3$ catalysts (19, 22).

Test Reactions

Table 4 also includes the values of initial activities for both test reactions: cyclohexane (CH) dehydrogenation (a structure-insensitive reaction) at 300°C and cyclopentane (CP) hydrogenolysis (a structure-sensitive reaction) at 400°C for monometallic and bimetallic catalysts. It can be observed that the tin addition to Pt/carbon produces an important decrease of dehydrogenation rate (approximately 10 times). Furthermore, the hydrogenolysis rate becomes negligible after tin addition. Besides, the activation energies of CH dehydrogenation for bimetallic catalysts strongly increase with respect to those of monometallic Pt catalysts. Taking into account that the CH dehydrogenation is a structure-insensitive reaction (which involves only one exposed site (24)), both the great drop of the specific activity and the important increase of the activation energy of PtSn catalysts with respect to Pt samples, indicate that a certain electronic interaction between both metals exists. The negligible catalytic activity for CP hydrogenolysis (a structure-sensitive reaction (25)) indicates that, in bimetallic catalysts, the Pt atoms ensembles required for this reaction are in a very low concentration. According to this, dilution and/or blocking effects of Sn on Pt particles would be associated to the alloy formation. However, the great Sn surface enrichment (≈20 Sn surface atoms per Pt surface atom) observed by XPS would indicate that an important amount of tin is blocking the surface of Pt particles. This blocking action of tin on Pt particles would inhibit the CH adsorption on each exposed metallic site in a very pronounced way, thus leading to a low CH dehydrogenation rate. It must be noted that Sn is inactive for CH dehydrogenation and CP hydrogenolysis reactions (2). However, the H_2-chemisorption is not affected in a similar extension, since it decreases only two times when tin is added to Pt (Table 4). This different behavior between CH dehydrogenation and H_2-chemisorption for bimetallic catalysts would be related with a higher steric restriction for CH adsorption than that for H_2 adsorption. These experimental findings can be explained considering a surface model where Sn is blocking both the alloy particles (which have a low activity for hydrogenation–dehydrogenation reactions (2)) and a fraction of the metallic Pt atoms. In this way some pairs of Pt atoms would be diluted by both alloy islands and oxidized tin.

The CH dehydrogenation reaction rates of monometallic catalysts (or bimetallic catalysts) supported on H_2O_2-functionalized carbon are higher than those of the corresponding catalysts supported on purified carbon (Table 4). These results would indicate a clear effect of the surface chemistry of the support in the catalytic activity. This behavior could be explained considering that, according to the literature (18), the oxygen surface groups could act as anchoring sites for the anionic platinum compound during the impregnation step, thus leading to a more external distribution of the active species on the carbon surface. Then, it can be suggested that in the case of catalysts prepared by using the nonfunctionalized support, the reaction could be partially hindered due to a low accessibility of the reactants to the Pt particles. A similar behaviour was observed in Pt catalysts supported on nonfunctionalized and functionalized carbons used in nitrobenzene hydrogenation reaction in liquid phase (26). It is worth to mention that the H_2-chemisorption on Pt/C-HP only increases about 12% with respect to that on Pt/C catalyst (Table 4). The lower effect of the functionalization treatment of the support on the H_2-chemisorption compared with the important modification of the catalytic activity in CH dehydrogenation can be assigned to a different accessibility between H_2 and CH molecules to the Pt particles.

Hydrogenation of Carvone

Carvone is a terpenic monocyclic ketone with three different functional groups able to be hydrogenated: an endocyclic −C=C− group, an exocyclic −C=C−, and a −C=O group. From the point of view of the chemical reactivity, the −C=C− bonds have different behavior than that of the −C=O group.

Figure 10a shows the activity (defined as the carvone conversion) as a function of the reaction time for monometallic Pt/C-HP and bimetallic PtSn/C-HP catalysts, prepared both by co-impregnation (C) and by successive impregnation

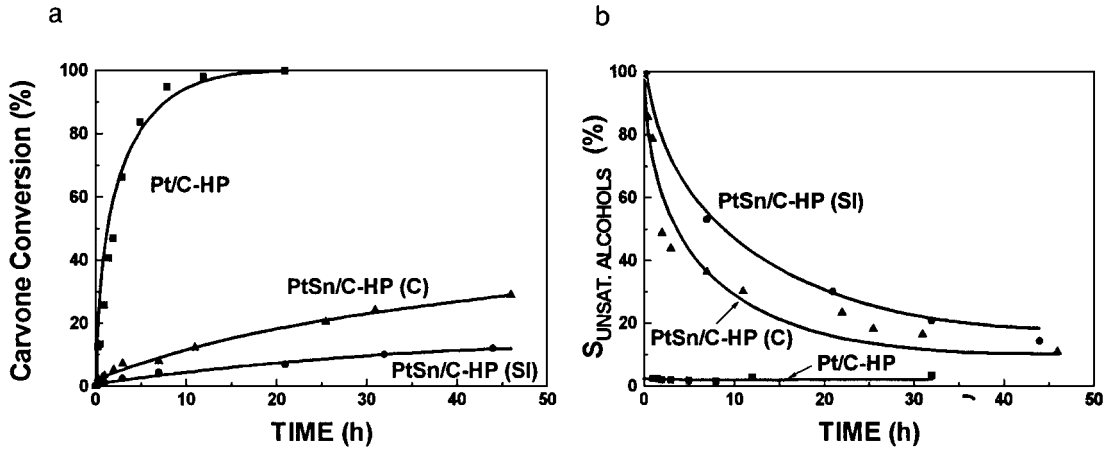

FIG. 10. Performance of different catalysts in the carvone hydrogenation reaction at 40°C: (a) carvone conversion as a function of the reaction time; (b) selectivity to unsaturated alcohols ($S_{\text{UNSAT. ALCOHOLS}}$) as a function of reaction time.

(SI). The monometallic catalyst shows an activity much higher than those of the bimetallic ones. Among the bimetallic PtSn catalysts, the sample prepared by co-impregnation is more active than the one prepared by the two-step impregnation.

In order to discuss the selectivity of the different catalysts, it must be considered that the catalytic carvone hydrogenation reaction can be described by the reaction scheme (27) shown in Fig. 11.

The selectivity to a given reaction product was defined as the amount of this product referred to the total amount of the different products. Besides, it must be indicated that the reaction products detected for these catalysts during the reaction time used in our experiments were only unsaturated ketones (mainly carvotanacetone) and unsaturated alcohols (carveol, the doubly unsaturated alcohol). Figure 10b shows the selectivity to unsaturated alcohols for the different catalysts. The Pt/C-HP sample displays a very high selectivity to unsaturated ketones over the whole range of the reaction time, and as a consequence the corresponding selectivity to unsaturated alcohols is very low (about 3–4%). It is well known that with supported monometallic catalysts, the selectivity to unsaturated alcohols is generally low, but it can be influenced by changes in the support, metal particle size, etc. (28). In this way, the selectivity of Pt catalysts supported on activated carbons is very different from that of Pt/Al_2O_3 catalyst, which is very active and produces almost only saturated ketones (27). In fact, the production of low amounts of unsaturated alcohols (carveol) observed for Pt/C catalysts (Fig. 10b) can be related to the effect of the support on the metallic phase. Figure 10b also shows that the selectivity to unsaturated alcohols of platinum catalysts supported on carbon is substantially enhanced by tin addition. According to the results shown in Fig. 10b, the difference in selectivity between both bimetallic catalysts prepared by successive impregnation (SI) or by coimpregnation (C) is not very important. From data of the Fig. 10b, it can be observed that the selectivity to carveol in PtSn catalysts is very high at low reaction times, reaching values very close to 100% at the beginning of the reaction, but it decreases at higher reaction times while carvotanacetone (the another reaction product) increases. It must be noted that carveol (the doubly unsaturated alcohol) is directly produced from hydrogenation of carvone, without intermediate steps (see Fig. 11).

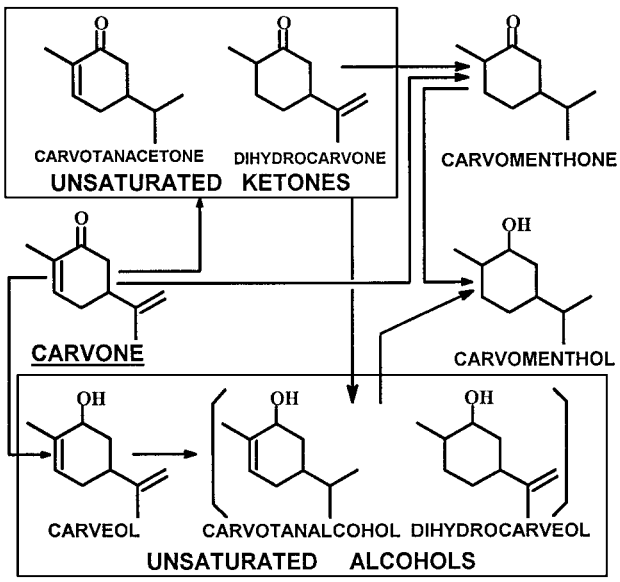

FIG. 11. Reaction scheme of carvone hydrogenation.

The carvone hydrogenation reaction on supported bimetallic catalysts was studied only by few authors (27, 29, 30). Jablonski *et al.* (27) reported a good selectivity to unsaturated ketones in this reaction for $PtSn/Al_2O_3$ catalysts. Besides, other authors found only the formation of

unsaturated and saturated ketones as intermediary products for Rh-supported catalysts (29) and for PtAu/SiO_2 (30). Results presented in this paper show that the most important changes in selectivity of bimetallic PtSn catalysts supported on carbon can be due not only to the action of the promoter (Sn) but also to the effect of the support (carbon). In this way, taking into account the characterization results of the metallic phase of these bimetallic catalysts, the high selectivity to unsaturated alcohols of PtSn/C-HP catalysts (prepared by both coimpregnation and successive impregnation) could be attributed to ionic tin associated with metallic platinum. These Sn ions deposited on the carbon surface would enhance the polarization of the carbonyl group, increasing the positive charge on the carbon atom of the −C=O group which can react easily with atomic hydrogen dissociated on the neighboring Pt particles. Besides, not only the formation of PtSn alloys but also the dilution of platinum by tin species, and the Pt blocking by Sn as well would produce the inhibition of the hydrogenation of the −C=C− bonds.

From these results, it can be inferred that when carbon is used as a support of Pt instead of alumina, the hydrogenation rates of the −C=C− bonds of carvone are strongly decreased, mainly that of the endocyclic −C=C− one, thus leading to the formation of carvotanacetone (unsaturated ketone). The Sn addition to Pt/carbon produces an additional effect. In this case, the hydrogenation of the −C=C− bonds appears to be retarded with respect to the hydrogenation of the −C=O bond. The hydrogenation of −C=O group is enhanced since this bond would be polarized by the presence of Sn ions in the vicinity of the Pt atoms.

CONCLUSIONS

(1) Sn/carbon samples can retain important amounts of H_2 during TPR experiments. The presence of both metallic tin and surface oxygen groups on the carbon are very important for the H_2 retention capacity of Sn catalysts.

(2) TPR profiles reveal the important differences in the metallic states of bimetallic PtSn catalysts compared to the monometallic ones.

(3) In PtSn/C samples most of Sn would be localized in the metallic phase of catalysts. As there are practically no free Sn species on the support, the H_2 retention at high temperatures may not take place.

(4) The surface of the reduced bimetallic catalysts, as revealed by XPS data, is composed of metallic platinum, Sn(II) and/or Sn(IV) species (about 85%), and also tin in the zerovalent state (about 15%) that, probably, is forming alloys with zerovalent platinum.

(5) The Sn surface enrichment (≈20 Sn surface atoms per Pt surface atom) observed by XPS would indicate that important amounts of tin are covering both the surface of Pt and the alloy particles.

(6) Bimetallic catalysts are less active than monometallic ones for CH hydrogenation and CP hydrogenolysis. The results indicate that deactivation produced by Sn addition occurs by electronic and/or geometric effects. Alloy formation and platinum surface blocking are suggested to interpret these phenomena.

(7) The use of carbon, instead of alumina, as a support of Pt produces an important modification not only on the activity but also on the selectivity in the carvone hydrogenation. A lower reactivity of the endocyclic −C=C− bond of carvone was found for Pt/C catalysts with respect to that for Pt/Al_2O_3, thus leading to a high selectivity to carvotanacetone. When Sn is added to Pt/C, an important additional effect was found on the selectivity. In this case, PtSn/C catalysts initially produce the doubly unsaturated alcohols as the main product. This fact reveals that the Sn addition to Pt/C inhibits the hydrogenation rate of −C=C− bonds and enhances the polarization of the −C=O bond of the carvone molecule, thus leading to carveol formation.

ACKNOWLEDGMENTS

This work was carried out in the context of the Intercampus Program between Universidad Nacional del Litoral (Argentina) and Universidad de Alicante (Spain). The financial support from the Secretary of Science and Technology (Universidad Nacional del Litoral) is gratefully acknowledged.

REFERENCES

1. Berndt, V. H., Mehner, H., Volter, J., and Meisel, W., *Z. Anorg. Allg. Chem*. **429**, 47 (1978).
2. Baronetti, G. T., de Miguel, S. R., Scelza, O. A., and Castro, A. A., *Appl. Catal.* **24**, 109 (1986).
3. Kuznetsov, V. I., Belyi, A. S., Yurchenko, E. N., Smolikov, M. D., Protasova, M. T., Zatolokina, E. V., and Duplyakin, V. K., *J. Catal.* **99**, 159 (1986).
4. de Miguel, S. R., Baronetti, G. T., Castro, A. A., and Scelza, O. A., *Appl. Catal.* **45**, 61 (1988).
5. Larsson, M., Andersson, B., Bariås, O. A., and Holmen, A., *Stud. Surf. Sci. Catal.* **88**, 233 (1994).
6. Cortright, R. D., and Dumesic, J. A., *J. Catal.* **157**, 576 (1995).
7. Merlen, E., Beccat, P., Bertolini, J. C., Delichere, P., Zanier, N., and Didillon, B., *J. Catal.* **159**, 178 (1996).
8. Passos, F. B., Schmal, M., and Vannice, M. A., *J. Catal.* **160**, 106 (1996).
9. Stagg, S. M., Querini, C. A., Alvarez, W. E., and Resasco, D. E., *J. Catal.* **168**, 75 (1997).
10. Padró, C. L., de Miguel, S. R., Castro, A. A., and Scelza, O. A., *Stud. Surf. Sci. Catal.* **111**, 191 (1997).
11. Coloma, F., Sepúlveda-Escribano, A., Fierro, J. L. G., and Rodriguez-Reinoso, F., *Appl. Catal. A* **136**, 231 (1996).
12. Coloma, F., Sepúlveda-Escribano, A., Fierro, J. L. G., and Rodriguez-Reinoso, F., *Appl. Catal. A* **148**, 63 (1996).
13. Pinxt, H. H., Kuster, B. F. M., Koningsberger, D. C., and Marin, G. B., *Catal. Today* **39**, 351 (1998).
14. Wagner, C. D., Davis, L. E., Zeller, M. V., Taylor, J. A., Raymond, R. H., and Gale, L. H., *Surf. Interface Anal.* **3**, 211 (1981).
15. de Miguel, S. R., Scelza, O. A., Román-Martínez, M. C., Salinas-Martínez de Lecea, C., Cazorla-Amorós, D., and Linares-Solano, A., *Appl. Catal. A* **170**, 93 (1998).

16. Román-Martínez, M. C., Cazorla-Amorós, D., Linares-Solano, A., and Salinas-Martínez de Lecea, C., *Carbon* **31**, 895 (1993).
17. Van Dam, H. E., and Van Bekkum, H., *J. Catal.* **131**, 335 (1991).
18. Román-Martínez, M. C., Cazorla-Amorós, D., Linares-Solano, A., and Salinas Martínez de Lecea, C., *Carbon* **33**, 3 (1995).
19. Baronetti, G. T., de Miguel, S. R., Scelza, O. A., Fritzler, M. A., and Castro, A. A., *Appl. Catal.* **19**, 77 (1985).
20. Calo, J. M., Cazorla-Amorós, D., Linares-Solano, A., Román-Martínez, M. C., and Salinas-Martínez de Lecea, C., *Carbon* **35**, 543 (1997).
21. Lau, C. L., and Wertheim, G. K., *J. Vac. Sci. Technol.* **15**, 622 (1978).
22. de Miguel, S. R., Castro, A. A., Scelza, O. A., Fierro, J. L. G., and Soria, J., *Catal. Lett.* **36**, 201 (1996).
23. Antonov, P. G., Nukushkin, Yu. N., Shtrele, V. G., Kostikov, Yu. P., and Egorov, F. K., *Zh. Neorg. Khim. SSSR* **27**, 3130 (1982).
24. Blakely, D. W., and Somorjai, G. A., *J. Catal.* **42**, 181 (1976).
25. Apesteguía, C. R., and Barbier, J., *in* "Proceedings of the VIII Iberoamerican Congress on Catalysis, Huelva, Spain," Malquiso, p. 751. 1982.
26. Torres, G. C., Jablonski, E. L., Baronetti, G. T., Castro, A. A., de Miguel, S. R., Scelza, O. A., Blanco, M. D., Jiménez, M. A. P., and Fierro, J. L. G., *Appl. Catal. A* **161**, 213 (1997).
27. Jablonski, E. L., Ledesma, S., Torres, G. C., de Miguel, S. R., and Scelza, O. A., *Catal. Today* **48**, 65 (1998).
28. Ponec, V., *Appl. Catal. A* **149**, 27 (1997).
29. Gómez, R., Arredondo, J., Rosas, N., and del Angel, G., *in* "Heterogeneous Catalysis and Fine Chemicals II" (M. Guisnet, *et al.*, eds.), p. 185. Elsevier Science Publishers B.V., Amsterdam, 1991.
30. del Angel, G., Melendrez, R., Bertin, V., Domínguez, J. M., Marecot, P., and Barbier, J., *in* "Heterogeneous Catalysis and Fine Chemicals III" (M. Guisnet, *et al.*, eds.), p. 171. Elsevier Science Publishers B.V., Amsterdam, 1993.